Impact of Neutrino Energy Reconstruction on Oscillation Experiments

CERN Summer Internship Report

12/09/2025

Supervisor: Dr. Stephen Dolan, Dr. Laura Munteanu

Author: Mara Pripon

Contents

1 Abstract

This report studies neutrino energy reconstruction and its effect on future long-baseline experiments such as DUNE and Hyper-Kamiokande (T2K). We examine the origin of energy biases arising from nuclear effects and reconstruction methods, and quantify their role in shaping oscillation measurements. Event rate predictions of Hyper-K and DUNE over a 10-year exposure are presented as a function of baseline length and true neutrino energy, including uncertainties from reconstruction. Finally, we discuss the prospects of the proposed nuSCOPE experiment, which would employ a tagged neutrino beam and a water Cherenkov detector to directly calibrate energy reconstruction for Hyper-K and measure neutrino cross-section with unprecedented precision, thereby reducing systematic uncertainties in future oscillation studies.

2 Introduction

2.1 Neutrino oscillations

Neutrinos are electrically neutral, extremely light fermions that belong to the lepton sector of the Standard Model, where they come in three flavors associated with the charged leptons (e, μ, τ). First postulated by Pauli in 1930 to explain missing energy in beta decay and later detected in 1956 by Cowan and Reines, neutrinos interact only via the weak force, making them notoriously difficult to detect.

Neutrinos are produced and detected as flavor eigenstates ($|\nu_\alpha\rangle$, $\alpha = e, \mu, \tau$), but propagate as a superposition of mass eigenstates ($|\nu_i\rangle$, $i = 1, 2, 3$). The relation between the two bases is given by the PMNS mixing matrix U,

$$|\nu_\alpha\rangle = \sum_{i=1}^{3} U_{\alpha i}^{*} |\nu_i\rangle \,. \tag{1}$$

After traveling a distance L with energy E, the probability of observing a flavor ν_β is

$$P(\nu_\alpha \to \nu_\beta) = \sum_{i,j} U_{\alpha i}^{*} U_{\beta i} U_{\alpha j} U_{\beta j}^{*} \exp\left(-i \frac{\Delta m_{ij}^2 L}{2E}\right), \tag{2}$$

where $\Delta m_{ij}^2 = m_i^2 - m_j^2$. Oscillations are therefore governed by the neutrino mass-squared differences, the mixing angles, and the CP-violating phase.

For illustrative purposes, in the two-flavor limit the transition probability reduces to

$$P(\nu_\alpha \to \nu_\beta) = \sin^2 2\theta \, \sin^2\left(\frac{\Delta m^2 L}{4E}\right), \tag{3}$$

with survival probability $P(\nu_\alpha \to \nu_\alpha) = 1 - P(\nu_\alpha \to \nu_\beta)$. The oscillation frequency depends on $\Delta m^2 L/E$, while the amplitude is controlled by the mixing angle θ, where $\Delta m^2 = m_2^2 - m_1^2$ and

$$\begin{pmatrix} \nu_e \\ \nu_\mu \end{pmatrix} = \begin{pmatrix} \cos\theta & -\sin\theta \\ \sin\theta & \cos\theta \end{pmatrix} \begin{pmatrix} \nu_1 \\ \nu_2 \end{pmatrix}. \tag{4}$$

Therefore, long baseline experiments that explore the oscillations of neutrinos are designed with a fixed L and various fluxes of energy that could probe the physics of the oscillations.

2.2 Neutrino interactions

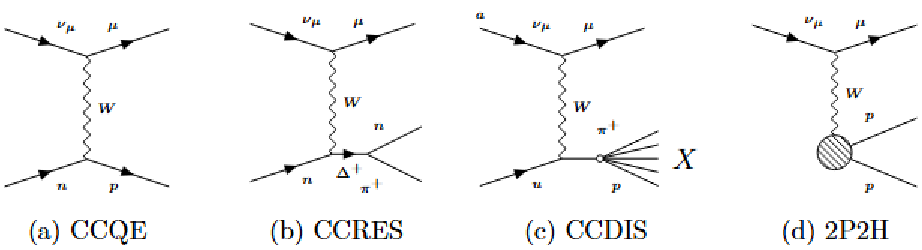

Figure 1: Neutrino Interactions Channels

As neutrinos are electrically neutral, their detection and energy reconstruction in oscillation experiments rely on their interactions with matter. Specifically, we focus on charged-current (CC) interactions, since the charged leptons they produce are directly coupled to the flavor of the incoming neutrino, thereby providing a way to tag the neutrino flavor and explore the oscillations.

Charged-current quasi-elastic (CCQE) interactions [Fig. 1(a)] correspond to scattering on a nucleon, producing a charged lepton and a recoiling nucleon. Charged-current resonant (CCRES) interactions [Fig. 1(b)] occur when the neutrino excites a nucleon into a Δ^+ or Δ^{++} resonance (typical for few-GeV scales), which subsequently decays into a nucleon and a pion (π^+ or π^0). At higher energies, charged-current deep inelastic scattering

(CCDIS) [Fig. 1(c)] proceeds via parton-level interactions with quarks inside the nucleon, producing pions, nucleons, and hadronic jets. Finally, two-particle–two-hole (2P2H) processes [Fig. 1(d)] involve the neutrino interacting with correlated nucleon pairs in the nucleus, leading to the emission of a charged lepton and two nucleons.

In addition to the different interaction channels, several nuclear effects play a crucial role in how neutrino interactions are observed in detectors. First, nucleons inside the nucleus are not at rest but carry a momentum distribution due to Fermi motion. Moreover, since nucleons are bound within the nuclear potential, part of the neutrino energy is used to overcome the binding energy, shifting the apparent kinematics compared to free-nucleon scattering. Finally, after the initial neutrino-nucleon interaction, the produced hadrons can undergo final-state interactions (FSI) while propagating through the nuclear medium, leading to re-scattering, absorption, or charge exchange. These effects can modify particle multiplicities and energies, and even alter the event topology seen in the detector. We will go through all of these effects in detail, as we study the energy reconstruction in two experiments. Altogether, such nuclear effects complicate the task of energy reconstruction and they represent an important source of systematic uncertainty in neutrino oscillation experiments.

3 Energy reconstruction study on DUNE and T2K

3.1 Role of Energy Reconstruction

In long-baseline accelerator neutrino oscillation experiments such as T2K and DUNE, the strategy relies on comparing neutrino interaction rates at a near detector, where oscillations are negligible, with those at a far detector, located hundreds of kilometers away, where oscillations are significant. The number of observed events of flavor ν_β, binned in reconstructed energy E_ν^{reco}, can be expressed as

$$N^{\nu_\beta}(E_\nu^{\mathrm{reco}}) \propto \; P_{\nu_\mu \to \nu_\beta}(E_\nu^{\mathrm{true}})\,\Phi(E_\nu^{\mathrm{true}})\,\sigma(E_\nu^{\mathrm{true}})\,\epsilon(E_\nu^{\mathrm{true}})\,S(E_\nu^{\mathrm{true}}, E_\nu^{\mathrm{reco}}), \tag{5}$$

where $P_{\nu_\mu \to \nu_\beta}(E_\nu^{\mathrm{true}})$ is the oscillation probability, $\Phi(E_\nu^{\mathrm{true}})$ is the flux spectrum at the source, $\sigma(E_\nu^{\mathrm{true}})$ is the neutrino interaction cross section, $\epsilon(E_\nu^{\mathrm{true}})$ is the detector efficiency, and $S(E_\nu^{\mathrm{true}}, E_\nu^{\mathrm{reco}})$ is the smearing function relating the true neutrino energy to its reconstructed value.

This expression highlights that the measured spectrum at the far detector depends on the reconstructed energy. If the assumed mapping between reconstructed and true neutrino energy, i.e. $S(E_\nu^{\text{true}}, E_\nu^{\text{reco}})$, is incorrect, there may be a bias in measurements of the oscillation parameters. Consequently, achieving a good understanding of the relationship between the reconstructed and true energy is essential for exploiting the full physics potential of future oscillation measurements.

Neutrinos are detected only via their interaction products. The incident neutrino energy must therefore be reconstructed from the measured energies and momenta of the outgoing particles. Depending on the detector technology employed, this can be done using:

- **Quasi-elastic kinematics**, where the neutrino energy is calculated from the outgoing lepton's angle and momentum under the assumption of a CCQE neutrino interaction with a single nucleon at rest. This is the typical assumption of T2K and Hyper-K.
- **Calorimetric methods**, summing the measured energies of all visible final-state particles, specific to experiments such as NOvA and MINERvA and the future DUNE experiment.

3.2 Fluxes

The schematic drawing in Fig.2 shows that protons are first accelerated and directed onto a target, producing a beam of mesons (pions, kaons) which are then selected by charge and focused into a decay volume. As these mesons decay, they generate a beam that is predominantly composed of muon neutrinos or antineutrinos. The composition and intensity of the beam are measured at a near detector, before neutrino oscillations can occur, and again at a far detector after oscillations have taken place.

The neutrino flux generated, $\Phi(E_\nu^{\text{true}})$, constitutes a key ingredient of Eq. 5. In the T2K experiment, a baseline of 295 km is combined with a narrow-band beam peaked around 0.6 GeV, tuned to the first oscillation maximum [Fig. 3]. In contrast, the DUNE experiment will employ a 1300 km baseline and a wide-band beam covering approximately 0.5–5 GeV, thereby spanning both the first and second oscillation maxima. In this case, neutrino energy reconstruction must remain accurate across a considerably broader range

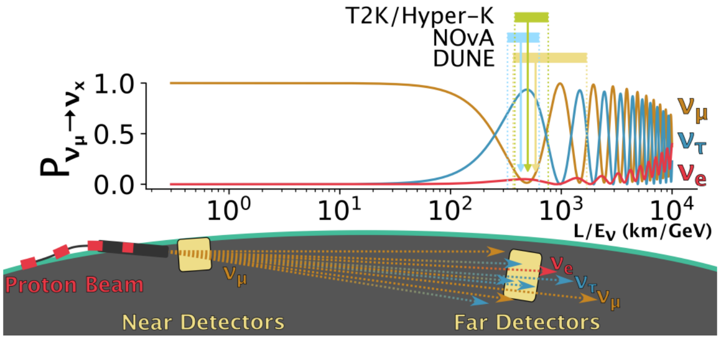

Figure 2: Schematic of an LBL neutrino oscillation experiment

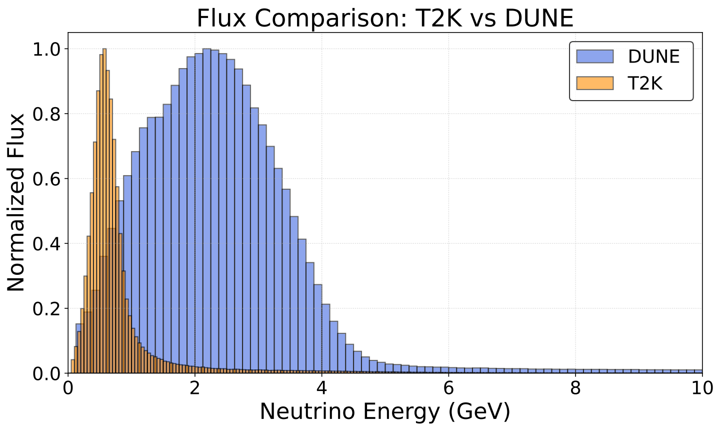

Figure 3: Fluxes of T2K and DUNE

of interaction channels, since the energy is increased.

Depending on the energy range and baseline, we can construct the plot in Fig. 2. It indicates the probability of observing an initially-produced muon neutrino as a particular flavour as a function of the ratio of L/E.

3.3 DUNE reconstruction of energy

Let us consider the difference between the true energy of the incoming neutrino and the energy reconstructed by the detector. For DUNE, we define

$$E_\nu^{\text{bias}} = E_\nu^{\text{true}} - E_{\text{had}}^{\text{vis}} - E_{\text{Lep}}, \tag{6}$$

- $E_{\text{had}}^{\text{vis}}$ is the visible hadronic energy, consisting of the kinetic energy of protons and charged pions, together with the total energy of neutral pions, electrons, and photons,
- E_{Lep} is the energy of the outgoing charged lepton.

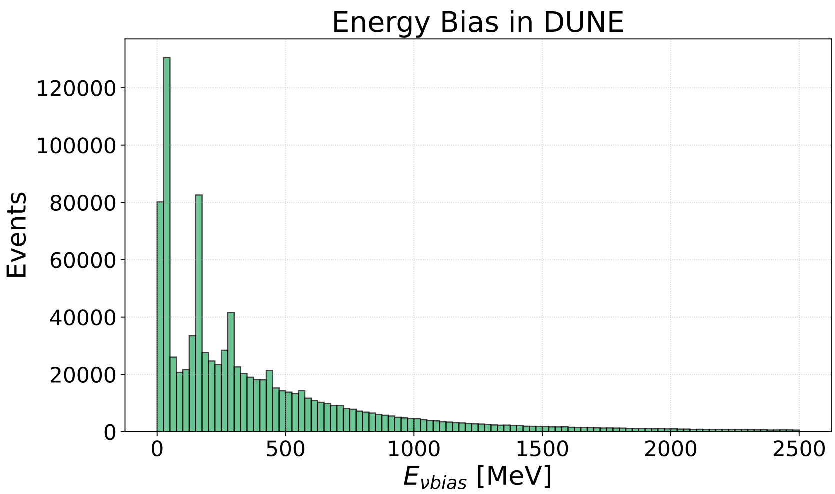

Figure 4: Plot of one million events generated and their absolute energy difference between the reconstructed and true value

It is important to note that the difference between the energies is always positive for DUNE [Fig. 4]. This is due to its method of computing the energy - summing every visible particle. So where can our biases come from? Clearly from possible outcomes that are very hard to detect or invisible for our detector, but there are several more subtilities that we need to analyze.

Firstly, the biggest peak shift from 0 comes as a consequence of binding energy. The shift is by $\approx 20MeV$. This occurs because the neutrino must supply additional energy to liberate a bound nucleon inside the nucleus before the interaction takes place.

3.3.1 Pion introduced biases

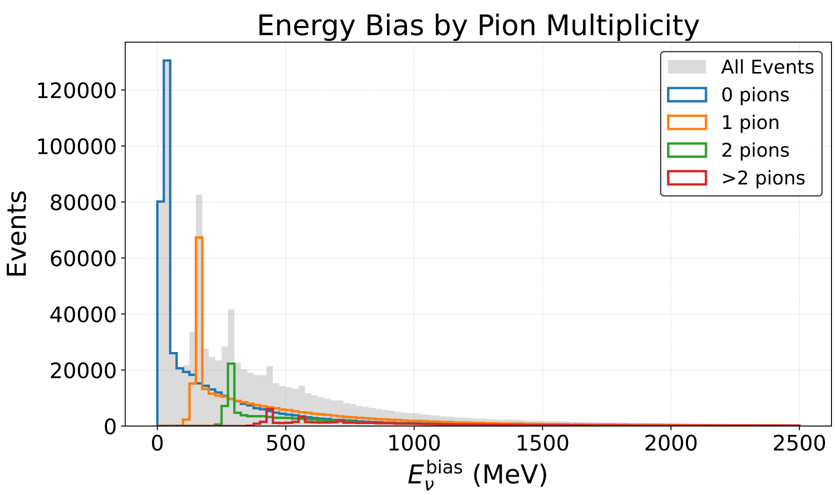

Figure 5: Events split by number of pions

The next peaks that we see in our absolute energy bias plot [Fig.5] are split by an energy value of $\approx 140MeV$ on average, which corresponds to the mass of a pion. Each peak has a width of the order of 50 MeV, which corresponds to the span in nucleon removal energies associated with the ground state of the nucleus. In the DUNE detector, charged pions can be identified through the tracks they leave as they propagate. However, once they come to rest, these pions decay into other particles, most notably producing neutrinos. The challenge is that the energy carried away by the neutrinos cannot be measured directly, and this "missing energy" corresponds precisely to the pion mass. In principle, if we could reliably determine the number of pion tracks present, their masses could be accounted for and reintroduced into the analysis. This correction, however, depends on having highly accurate reconstruction capabilities.

3.3.2 Neutron events impact on bias

The tail of the energy bias, highlighted in Fig. 6, comes from events involving neutrons—neutral particles that are largely invisible in DUNE. These neutrons can originate from several sources: they are produced in the initial neutrino interaction (for example, in CCRES [Fig. 1(b)]) or as secondary particles from the interactions of other hadrons inside the detector or appear in final state interactions. Because DUNE cannot directly detect these neutral particles, the energy they carry contributes to the largest source of bias in the reconstructed energy.

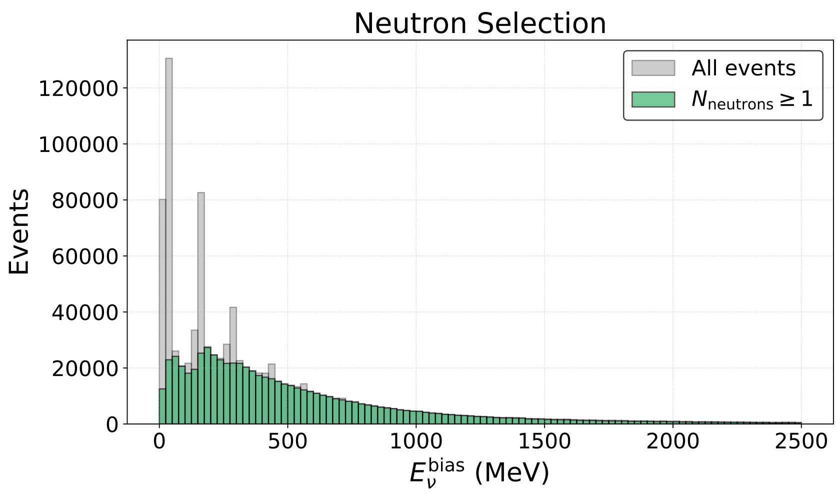

Figure 6: Tail in the energy bias plot made of events that contain neutrons

3.3.3 Relative Energy bias

The relative energy bias becomes important in order to understand the magnitude of the biases. Its equation is:

$$\text{Relative Energy Bias} \;=\; \frac{E_\nu^{\text{true}} - E_\nu^{\text{reco}}}{E_\nu^{\text{true}}}. \tag{7}$$

In the relative energy bias plot [Fig. 7], we notice that most of the bias comes from the 2P2H, resonant and deep-inelastic scattering interaction channels. However, 75% of the events have a bias of less than 20%.

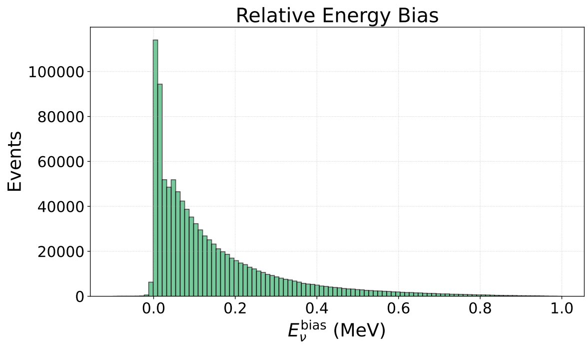

Figure 7: Relative energy bias in DUNE

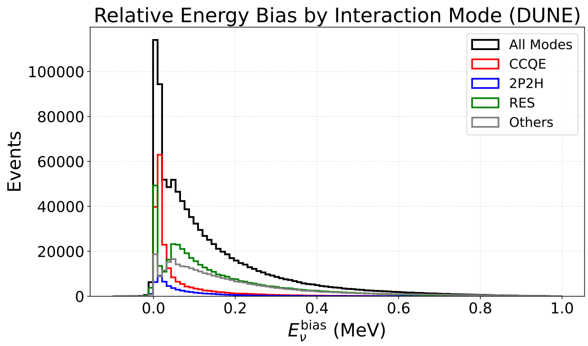

Figure 8: Relative energy bias by interaction channel in DUNE

3.3.4 T2K Energy Reconstruction

Experiments such as **T2K** and **Hyper-K** record the majority of their neutrino flux below 1 GeV, where interaction channels are predominantly characterized by *pionless final states*. The detectors mainly observe the outgoing leptons and pions produced in neutrino interactions.

In this context, the primary observable used to infer the neutrino energy is the *quasi-elastic (QE) reconstructed energy*, defined as

$$E_{\nu,\text{QE}}^{\text{rec}} = \frac{m_p^2 - m_\ell^2 - (m_n - E_B)^2 + 2E_\ell(m_n - E_B)}{2\big(m_n - E_B - E_\ell + p_\ell^z\big)}, \tag{8}$$

where m_p, m_ℓ, and m_n are the proton, outgoing lepton, and neutron masses, respectively (with proton and neutron masses interchanged for antineutrino interactions). The terms E_ℓ and p_ℓ^z denote the *energy* and *longitudinal momentum* (along the incoming neutrino direction) of the outgoing lepton, and E_B is a fixed nuclear binding energy of the struck nucleon (taken as 25 MeV for carbon in this work, as the near detector in T2K is made of carbon). The far detector is made of water, with a different nuclear binding energy. DUNE, however, has both detectors made from liquid argon, keeping the same bias in both detectors.

This expression is derived under the assumption of a *charged-current quasi-elastic (CCQE)* interaction on a stationary nucleon target, producing a single proton in the final state. It serves as an example of *kinematic neutrino energy reconstruction*, and is typically used by Water Cherenkov Detectors. We see in Figure 9 how significant the biases are in the all charged-current events hypothesis. To reduce the biases, T2K considers only charged current events with 0 pions.

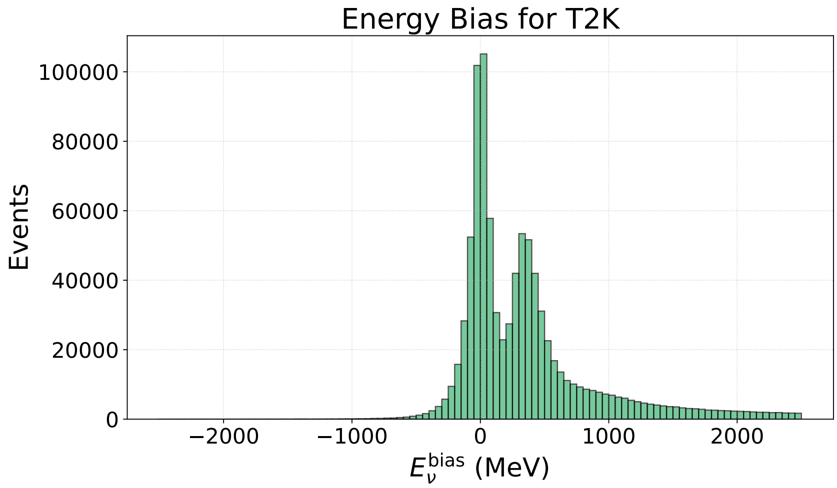

Figure 9: Energy bias plot for T2K

3.3.5 Quasi-elastic interactions vs. 0 Pions Selection

To mimic the CCQE events [Fig. 10], T2K selects events with no pions [Fig. 11], which are dominated by CCQE interactions. However, we have a contamination of non-CCQE events that absorbed the pions produced in the nucleus (after the neutrino nucleon interaction), becoming undetectable.

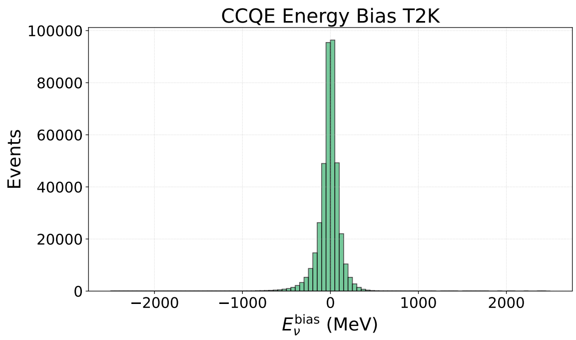

Figure 10: CCQE Energy Bias

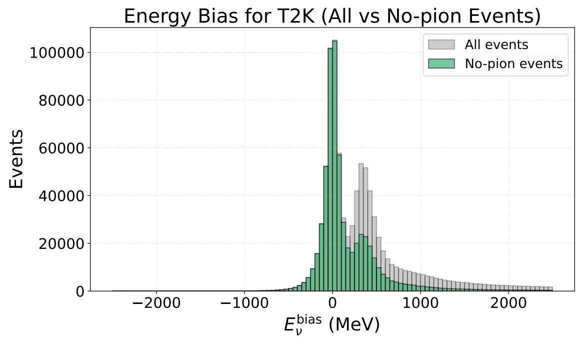

Figure 11: No Pions selection impact

Notice in [Fig. 12] how the peak is not centered in 0, but rather shifted with an amount of $-7.5MeV$. This is due to to binding energy - in reality the binding energy is not fixed, unlike in the equation we use to reconstruct the energy. The spread is due to Fermi motion, as inside the nucleus, nucleons are moving with momenta up to a few hundred MeV/c due to the Fermi momentum distribution.

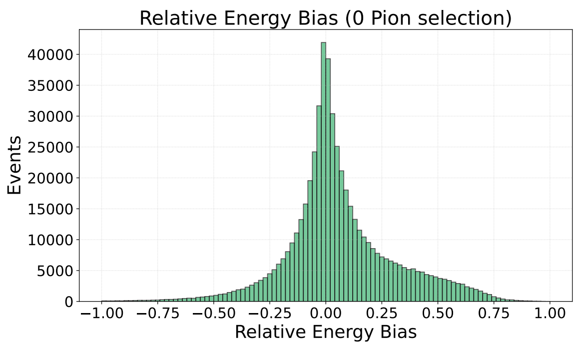

Figure 12: Relative Energy bias, No pion selection

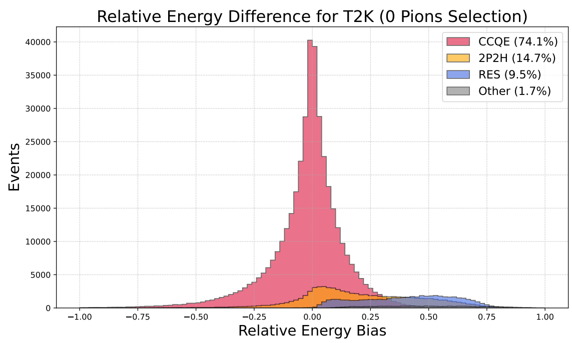

Figure 13: Relative Energy bias, split by interaction channels

From plotting the relative energy bias, T2K has 71% of the generated events with bias less than 20%.

Finally, we take a look at the normalized relative energy bias for both the experiments to notice their features - one-sided plot for DUNE vs almost-symmetric with respect to 0 energy bias for T2K [Fig. 14].

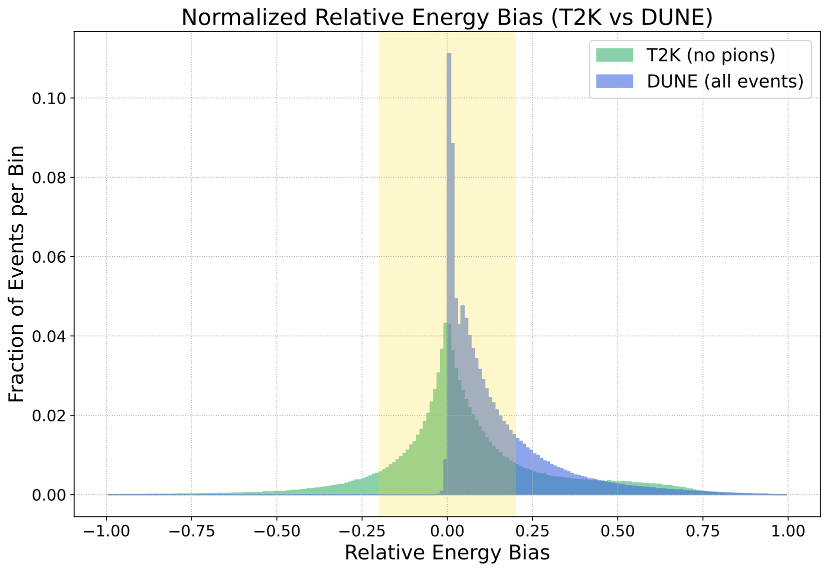

Figure 14: Comparison of normalized relative energy bias

3.4 No Final State Interactions Study

Hadrons produced in the primary neutrino–nucleon interaction must propagate through the nuclear medium before leaving the target nucleus. During this propagation they can undergo *final state interactions* (FSI), which significantly alter the observable final state. Typical processes include pion absorption, charge exchange, and elastic scattering, as illustrated in Fig. 15. In the following study, we are using a simulation where FSI are turned off, in order to isolate their effect on the neutrino energy bias.

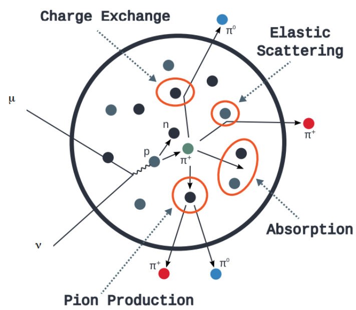

Figure 15: Illustration of hadronic final state interactions inside the nucleus, Img. from 2

3.4.1 No FSI in DUNE

Figure 16 we have the energy bias of events with no final state interactions, where we notice again the feature of the peaks produced by the number of pions in interactions [Fig. 17].

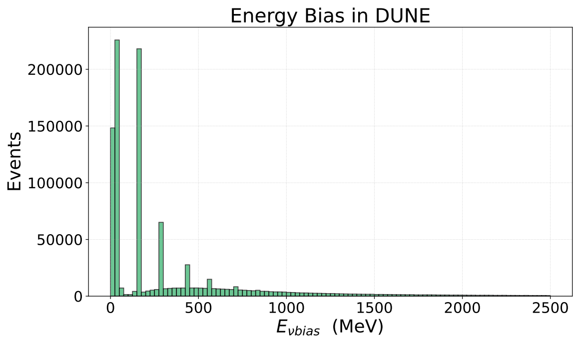

Figure 16: Energy bias in DUNE.

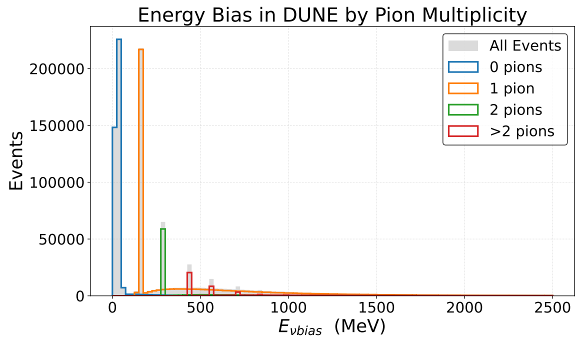

Figure 17: Energy bias with pion contributions.

In the no final state interactions selection, DUNE loses most of its tail - events with neutrons are reduced by 60% [Fig. 18]. This shows that most of the neutrons that impact the energy bias are produced in final state interactions

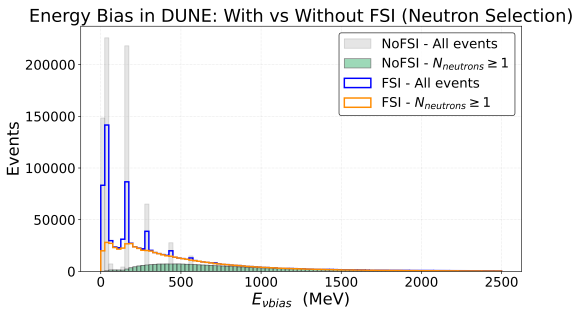

Figure 18: Impact of FSI on energy bias

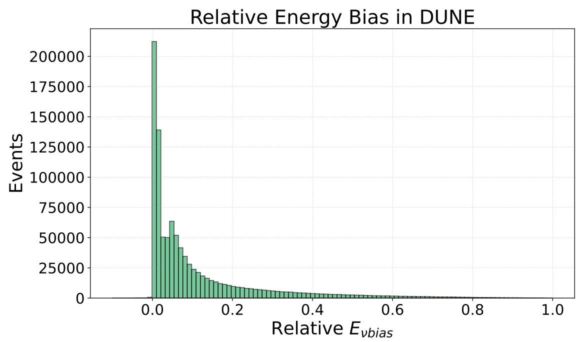

Figure 19: Relative energy bias.

81.6% of the events have a bias less than 20%, with the relative energy bias dropping abruptly, as seen in Fig.19.

3.4.2 NO FSI IN T2K

In 20 and 21 we see the differences between the energy bias of FSI included and No FSI simulation. In the

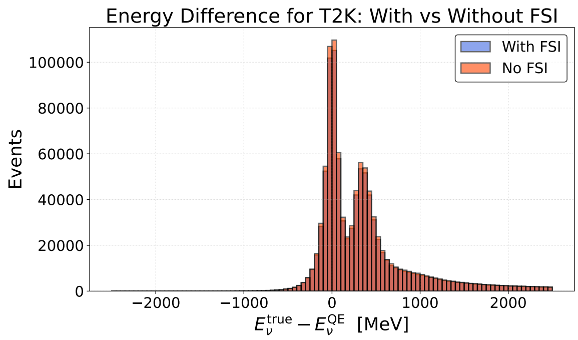

Figure 20: Energy difference in T2K including FSI effects.

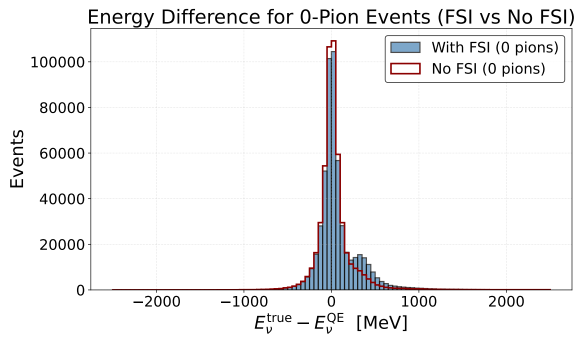

Figure 21: Energy difference in T2K for 0π final states.

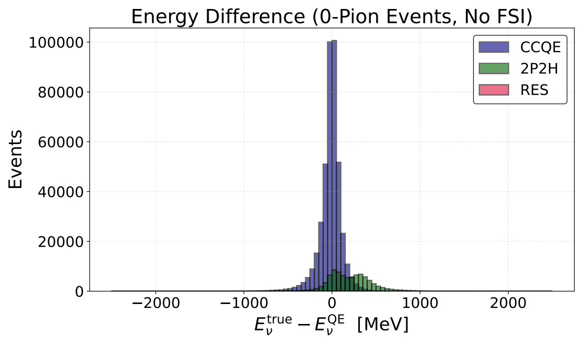

Figure 22: Energy Bias in no FSI and no pions T2K events

The only interaction channels in no pion selection, no final state interactions are CCQE 84% and 2P2H 16% (small contamination, as the pion is being absorbed).

In no FSI, T2K loses the bias coming from the resonant interactions [Fig.22]. However, they were already not imposing a significant bias, as we see in Fig. 13, where only 9.5% of the events in the relative energy bias plot are from resonant interactions. Therefore, FSI impacts T2K less than it does with DUNE.

4 L/E Study on DUNE and Hyper-K

4.1 Study of L/E

In this part, we conduct a study of how the next-generation LBL experiments DUNE and Hyper-K perform statistically as function of the ratio of the length of the baseline to the neutrino energy L/E, while understanding how precise the measurements are through energy resolution. We study the event rates of muon neutrino events happening in 10 years, as the experiments predict their number of events (ref. at 3 and 4). The plot is shown in [24]

Experiment	T2K	NOvA	Hyper-K	DUNE
Baseline (km)	295	800	295	1300
$N^{FD}_{\nu_\mu}$ (ν-mode)	318	211	≈9000	≈15000
$N^{FD}_{\bar{\nu}_\mu}$ ($\bar{\nu}$-mode)	137	125	≈12000	≈8000

Figure 23: Event rates for Hyper-K and DUNE corresponding to 10 years data

We are especially interested in how sensitive the two experiments are in different regions of energy. Oscillation dips are clearly visible near $L/E \sim 500$ km/GeV, and for DUNE, a second dip appears around $L/E \sim 1250$ km/GeV. The higher statistics and broader L/E coverage in DUNE allow for the exploration of neutrino oscillations over a full oscillation period, providing sensitivity to potential new physics effects.
Hyper-K has a significantly lower baseline (295 km) and a limited range of neutrino energy , which channels the event rates around the first oscillation dip only.

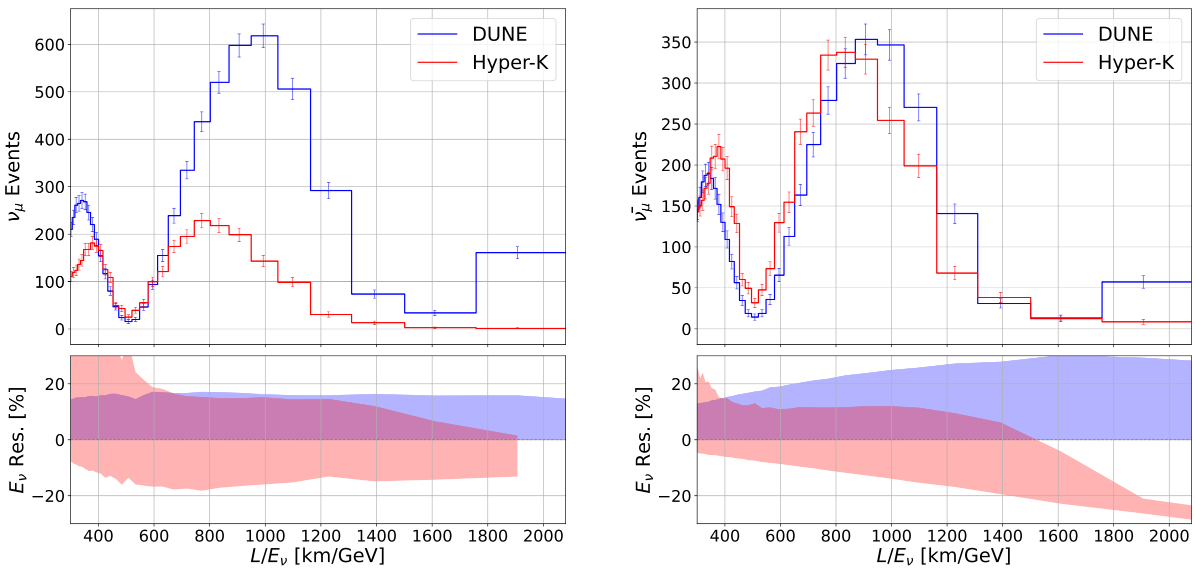

Figure 24: Study of event rate of muon neutrino and muon anti-neutrino in DUNE and Hyper-K, with corresponding energy resolution

The energy resolution of each experiment is characterized differently, as we showed in the previous part. For DUNE, the resolution is quantified using the 68th percentile of the relative difference between true and reconstructed neutrino energy,

$$\frac{E_\nu^{\text{true}} - E_\nu^{\text{reco}}}{E_\nu^{\text{true}}}. \tag{9}$$

For Hyper-K, the resolution is described using the 34th percentiles of the positive and negative relative energy bias.

We notice poor energy resolution in low L/E range for Hyper-K, as the CCQE assumption at high energies can no longer hold. DUNE seems to hold an advantage, as the energy resolution is one-sided.

However, in the anti-neutrino event rate plot, the two experiments behave similarly. DUNE has lower statistics in the anti-neutrino sector. As reminder, in CCQE interactions: $\bar{\nu}_\mu + p \rightarrow \mu^+ + n$. This makes the energy resolution worse in DUNE, as neutrons are not spotted easily in this experiment.

In these plots, the nominal DUNE and Hyper-K run plans are different: DUNE will have 1:1 ratio neutrino: to antineutrino, while Hyper-K will have a 1:3 ratio. However, we notice in the plot 24 that Hyper-K does not necessarily have more statistics, contrary to what was expected, but it has better energy resolution than DUNE for its region of interest.

5 Future Experiment NuSCOPE - Feasibility of a Water Cherenkov Detector

The future experiment nuSCOPE [1] proposes to perform high precision measurements of neutrino cross-sections, which can help reduce the uncertainty on the biases that affect DUNE and Hyper-K. The planned nuSCOPE ability of measuring neutrino energy on an event-by-event basis provides a substantial improvement over conventional techniques. With percent-level accuracy in both energy determination and flux normalization, neutrino–nucleus cross-section measurements could achieve a precision comparable to that of electron–nucleus cross-sections experiments, thereby reducing systematic uncertainties in oscillation studies.

A key feature is neutrino tagging, which enables the determination of the neutrino energy on an event-by-event basis by correlating the detected neutrino with its parent particle. Combined with beam monitoring at the level of 1% flux uncertainties, this tagging capability significantly reduces systematic errors. nuSCOPE is designed to operate over a wide energy range, covering the regions relevant for both DUNE and Hyper-Kamiokande. These performances rely on a slow-extraction, low-intensity beam, large detectors of order of kilotons positioned close to the decay tunnel, and excellent timing resolution in both the beamline and detectors.

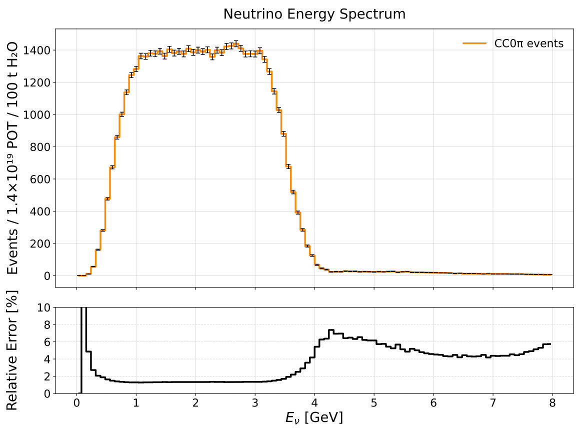

Figure 25: CC0pi muon neutrino event rate

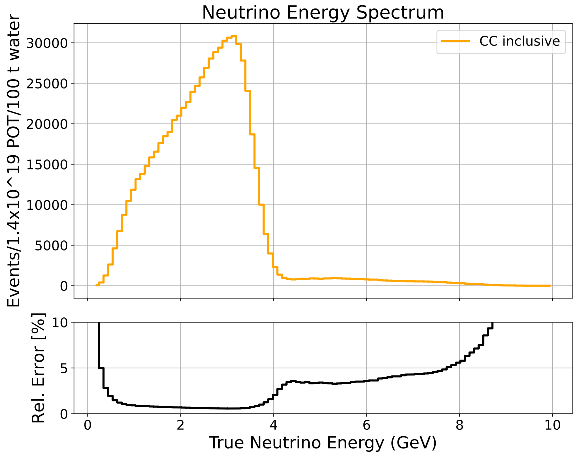

Figure 26: CC-inclusive total muon neutrino event rate

Water is the target material for Hyper-Kamiokande, making a detector based on this target an invaluable tool for achieving the nuSCOPE physics goals through precise neutrino interaction measurements in water. This final part of the report focuses on a preliminary study of the dimensions of a water cherenkov detector designed for this. In this study, we consider a 100 tons fiducial volume WC detector, positioned 25m from the end of the decay tunnel. The front face measures $4 \times 4m^2$.

We generate 1 million CC-events of muon neutrino. The total number of expected events in nuSCOPE is obtained by multiplying the flux integral and the corresponding cross section, and scaling this number according to the expected exposure, i.e. 1.4×10^{19} PoT, and the number of nucleons in the detector volume.

The total CC events and CC 0 pions events are presented in Fig.25 and Fig.26. We manage to tag 1.4×10^5 muon neutrino CC events, out of which 52×10^3 are tagged muon neutrinos CC 0 pions events.

5.1 Total cross-section measurements

In neutrino experiments, the number of observed events comes from the convolution of the incoming neutrino flux with the interaction cross section. Using a tagged neutrino beam, this makes the measurement of the total cross section in Fig.27 and 28 (with units of cm^2/nucleon) to be easily measured from the tagged neutrino events:

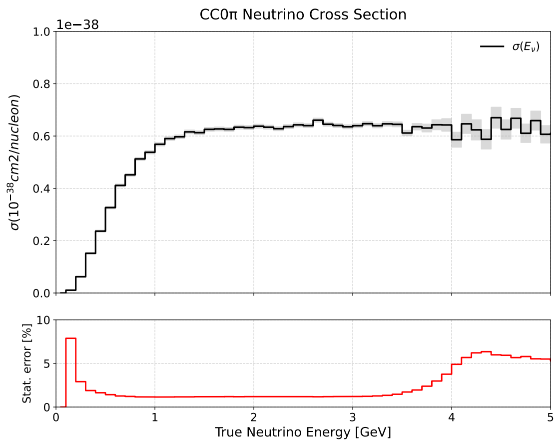

Figure 27: CC 0 pions selection neutrino cross section

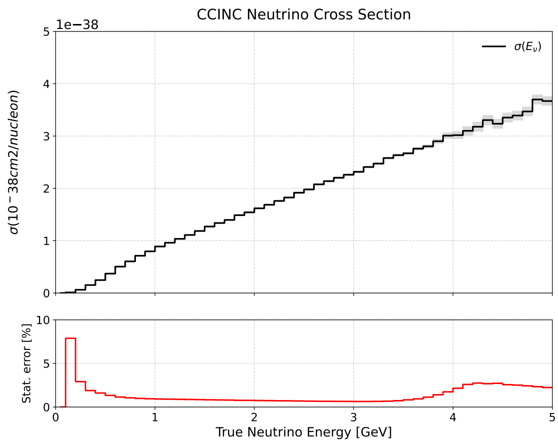

Figure 28: CC inclusive selection neutrino cross section

$$\sigma = \frac{N_{\text{events}}}{\Phi\, N_{\text{tgt}}\, N_{\text{PoT}}}, \tag{10}$$

where N_{events} is the number of expected signal events in the detector (what we plotted in Fig. 25), Φ is the neutrino flux (in units of $\nu/\text{cm}^2/\text{PoT}$), N_{tgt} is the number of nucleons in the fiducial volume, and N_{PoT} is the total proton-on-target exposure, here taken as 1.4×10^{19} PoT.

Notice that because of the large detector assumed in the setup, we managed to get statistical errors associated with the measurements to be less than 2% on most of the region of interest for Hyper-K.

5.2 Calibration measurements - Measuring the neutrino energy bias

nuSCOPE would make it possible to measure directly the neutrino energy bias thanks to its tagged reference neutrino beam, providing important constraints for future LBL experiments.

The expected event rates as a function of the relative neutrino energy bias is shown in Fig.29.

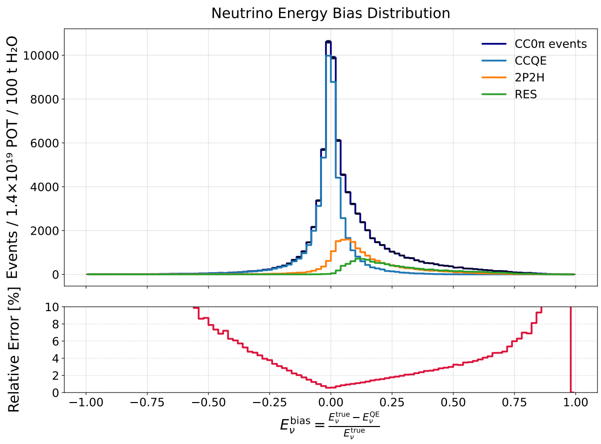

Figure 29: Event Rates as function of neutrino energy bias

In 6 we have the projected measurement of the relative neutrino energy for different regions of neutrino energy with a tagged neutrino beam and within the relevant energy. The energy ranges are within $0 - 4GeV$ with a step of $500MeV$. We notice that in the region of interest for Hyper-K, the relative energy bias measurement can be made with a statistical precision below 4% across the entire range.

As a conclusion, with a tagged neutrino beam and within the relevant energy ranges, one can not only disentangle the components of neutrino interaction models, but also use these measurements to calibrate the energy bias in Hyper-K's far detectors as a function of neutrino energy across the full range of interest.

5.3 Oscillation analysis

The aim of this final section is to compare the statistical errors expected in nuSCOPE (with a respective 100t and 200t detector) to the ones that Hyper-K expects to have in its far detector samples.

In Fig. 30, we have the statistical errors of a corresponding 100t nuSCOPE detector and Hyper-K. NuSCOPE is generally perfoming better with an error of less than 5%, except the region up to $500MeV$.

In Fig.31 we notice a reduction of statistical errors from nuSCOPE as we increase the detector size by 200t. The nuSCOPE error in the region of interest of Hyper-K drops to below 3%, performing significantly better than Hyper-K in that range.

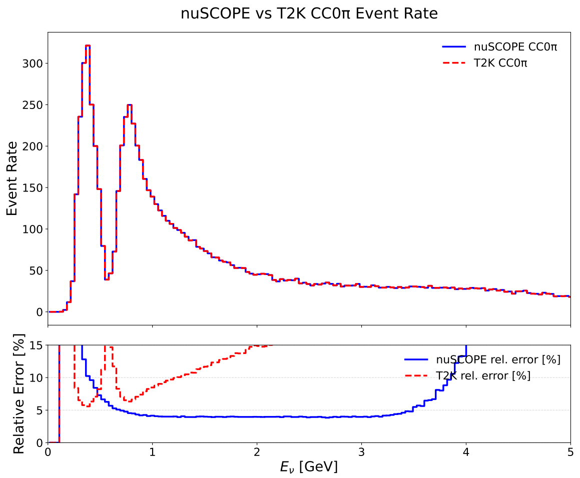

Figure 30: 100t detector

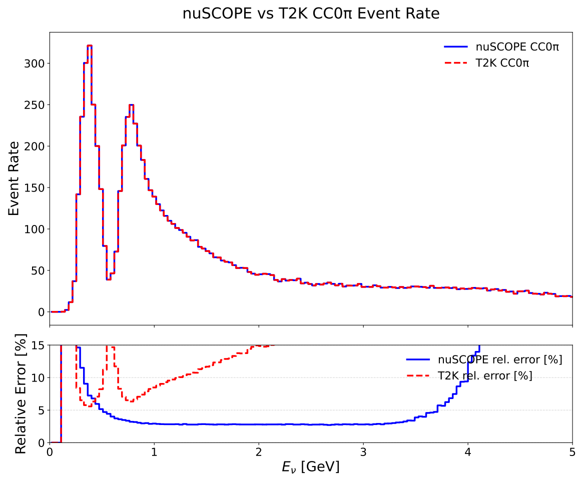

Figure 31: 200t detector

Figure 32: Comparison of statistical errors in the event rates of nuSCOPE and Hyper-K

6 Conclusions

In this work we have investigated how neutrino energy reconstruction impacts future long-baseline oscillation experiments such as Hyper-K and DUNE. By comparing calorimetric and kinematic methods, we showed that biases in the energy reconstruction arise from different physical origins: pion production and missing neutrons dominate in DUNE's calorimetric approach, while CCQE interactions assumption drive the bias in T2K's kinematic method. We have taken a look at how final state interactions influence DUNE's energy bias more than T2K's. Our L/E studies further emphasize the complementarity of wide-band (DUNE) and narrow-band (Hyper-K) beams in accessing oscillation physics. Looking ahead, we highlight the potential of nuSCOPE to provide direct experimental constraints on neutrino–nucleus interactions and to calibrate energy reconstruction with unprecedented precision. Such measurements are crucial for reducing systematic uncertainties and for enabling the next generation of oscillation experiments to achieve their ultimate goals: resolving the neutrino mass ordering and establishing leptonic CP violation.

Annexes

nuSCOPE WC Detector Study: Energy Bias Spectrum split in ranges of true neutrino energies

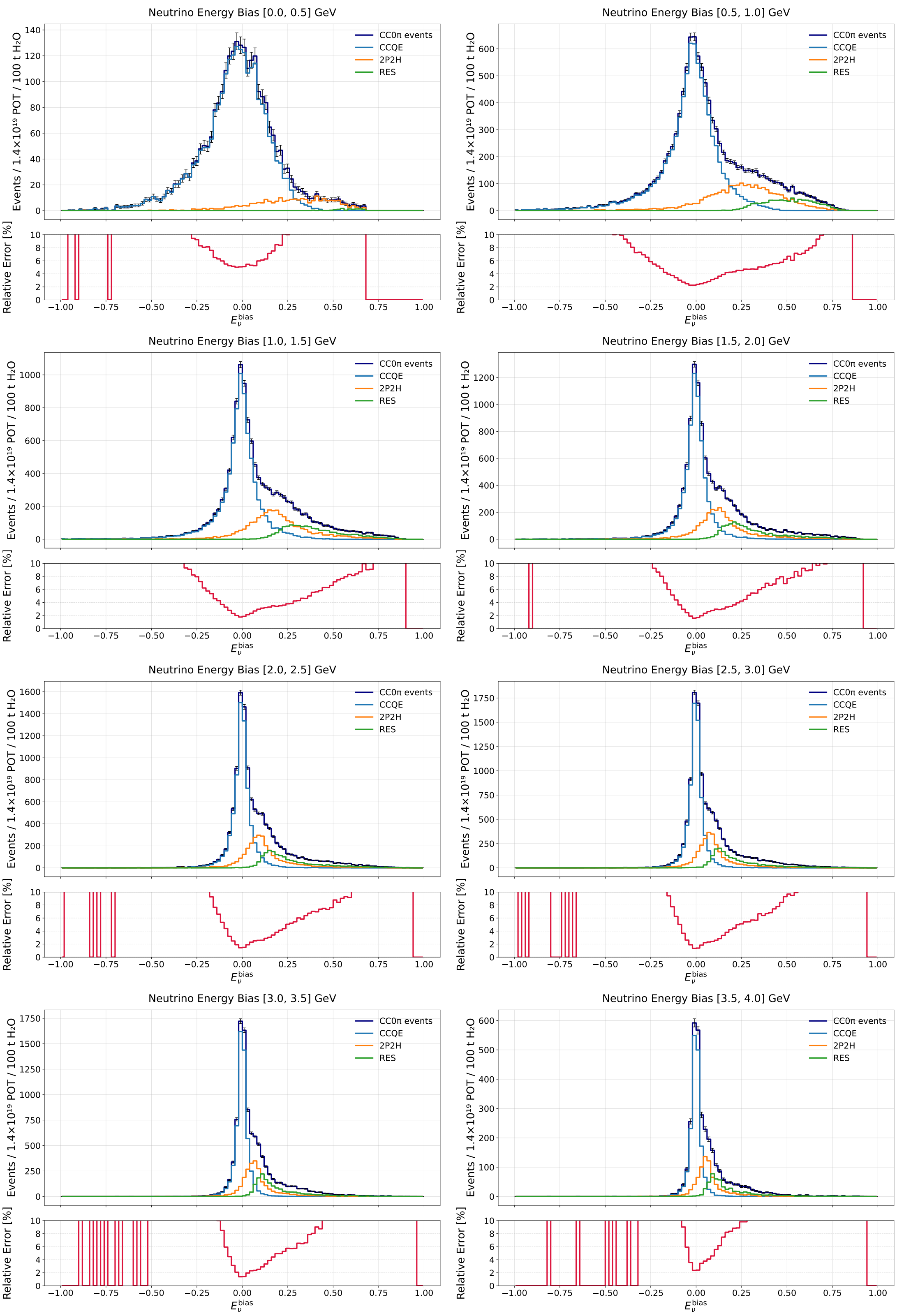

Figure 33: Energy Bias Spectrum split in ranges of $500 MeV$

References

1. nuSCOPE: A short-baseline neutrino beam at CERN for high-precision cross-section measurements, F.Acerbi et al., 2025, paper,

2. NuSTEC White Paper: Status and Challenges of Neutrino-Nucleus Scattering, L.Alvarez-Ruso et Al., 2017, paper,

3. Sensitivity of the Hyper-Kamiokande experiment to neutrino oscillation parameters using acceleration neutrinos, Hyper-Kamiokande Collaboration, 2025, ,

4. Low exposure long-baseline neutrino oscillation sensitivity of the DUNE experiment, DUNE Collaboration, 2021, ,